Masson *et al. Earth, Planets and Space* (2024) 76:114
https://doi.org/10.1186/s40623-024-02060-1

Earth, Planets and Space

FULL PAPER

Open Access

The pioneer Cluster mission: preparation of its legacy phase near re-entry

Arnaud Masson[1*], C. Philippe Escoubet[2], Matthew G. G. T. Taylor[2], Detlef Sieg[3], Silvia Sanvido[4], Beatriz Abascal Palacios[5], Stijn Lemmens[3] and Bruno Sousa[3]

Abstract

The Cluster mission will always be the first ever multi-spacecraft mission mapping the Earth magnetosphere in three dimensions. Launched in 2000 and originally planned to operate for two years, it has been orbiting Earth for more than two solar cycles. Over the course of its lifetime, its data have enabled the scientific community to conduct pioneer science. Recent scientific highlights will be presented first, followed by the latest scientific objectives that have guided the Cluster mission operations from 2021 until 2024. Early September 2024, one spacecraft of this veteran constellation will re-enter in a controlled manner the Earth's atmosphere, followed by its companions in 2025 and 2026. As we will see, this will be a unique opportunity to improve the ESA space debris re-entry models. Lastly, preparation of its legacy phase will be presented.

Keywords Magnetosphere, Cusp, Magnetotail, Magnetopause, Magnetosheath, Bow shock, Auroral plasma physics, Multi-spacecraft, Cluster

*Correspondence:
Arnaud Masson
Arnaud.Masson@esa.int
Full list of author information is available at the end of the article

Graphical Abstract

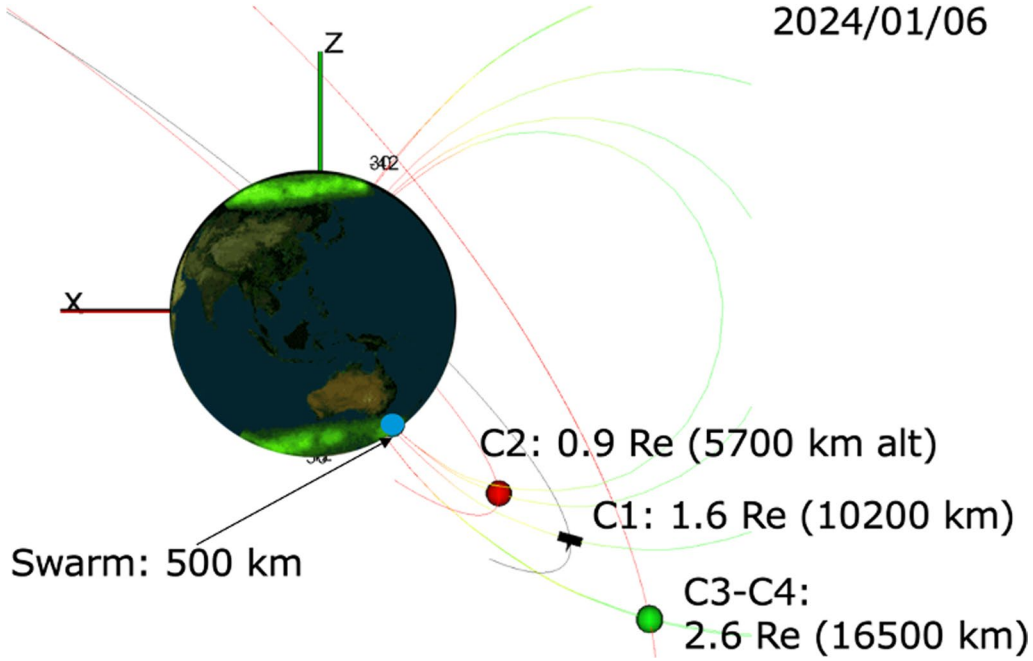

1 Introduction

The Cluster mission is a mission of international collaboration between the European Space Agency (ESA) and NASA (Escoubet et al. 2001). It is composed of four identical spacecraft, launched in summer 2000, into an Earth centric polar orbit between 4 Earth radii (R_E) and 19.6 R_E. Each satellite is equipped with a complete suite of 11 in situ plasma instruments measuring electromagnetic fields from DC to a few hundreds of kHz and particles from a few eV to MeV energies.

Cluster is the first ever multi-spacecraft mission flying in constellation and mapping our Earth's magnetosphere in 3D at fluid and ion scales. Since its launch, it has been joined by other spacecraft constellation like the NASA Time History of Events and Macroscale Interactions during Substorms (THEMIS) in 2007 (Angelopoulos 2008), the ESA Swarm ionospheric mission in 2013 (Friis-Christensen 2008) and the NASA Magnetospheric MultiScale (MMS) mission in 2015 (Burch et al. 2016). Together with Geotail (Nishida 1994), the Van Allen Probes (Mauk et al. 2013) and Arase (Miyoshi et al. 2017), they form a constellation of single spacecraft missions and spacecraft constellations, allowing system level science of the magnetosphere.

As of March 2024, the data collected by the Cluster mission have enabled the publication of more than 3200 refereed papers, 120 PhD and 30 master theses. A detailed analysis of these publications, together with a selection of scientific highlights over the first 20 years of Cluster operations, are presented in Escoubet et al. (2021). The present paper can be considered as a follow-up of Escoubet et al. (2021).

In Sect. 2, we will evoke a few scientific nuggets published since then. These results are related to space weather science, multi-scale plasma physics, auroral plasma physics and citizen science, and more unexpectedly, to Lunar and Martian science. Some take advantage of planned conjunctions with other spacecraft constellations like Swarm, MMS, or THEMIS. Others make use of decades of measurements, sometimes combined with innovative approaches like machine learning.

Section 3 presents the latest scientific objectives of the Cluster mission from 2021 until the end of its operations (September 2024). While agreed by the Science Operations Working Group,[1] endorsed by the ESA scientific advisory committees and eventually the ESA Science Programme Committee (SPC), these objectives have never been presented into a refereed paper.

[1] The Cluster SOWG is composed of all the experiments Principal Investigators, the Science Operations Center members located in the Rutherford Appleton Laboratory, and ESA.

Section 4 discusses the re-entry of the first Cluster spacecraft in the Earth's atmosphere and the scientific benefits expected. The last section will discuss the preparation of its legacy phase.

2 Recent scientific highlights

2.1 Space weather science

2.1.1 Cluster and Swarm link GICs to bursty bulk flows

Strong geomagnetically induced currents (GICs) can highly impact key human infrastructures, from corroding oil and gas pipelines (Gummow and Eng 2002) to causing complete outage of high-voltage power system (Boteler et al. 1998), as experienced in March 1989 in Canada (Bolduc 2002). GICs result from rapid variations of the Earth's magnetic field on the ground, or dB/dt. But what is the source of these fluctuations? Wei et al. (2021) reported that Earth-directed short-lived ion flows from the magnetotail, named bursty bulk flows (BBFs), can be linked to intense dB/dt. This paper details a case study, in early January 2015, when a fortuitous conjunction occurred between Cluster and the Swarm missions, during a geomagnetic storm. Both spacecraft constellations were magnetically linked to the same region in north America, supplemented with ground-based magnetometers from the SuperMAG network (Gjerloev 2009, 2012). Multiple BBFs were observed by Cluster in the magnetotail while Field Aligned Currents (FACs) were detected by Swarm in the ionosphere at around 400–500 km altitude, together with intense dB/dt seen by SuperMAG on the ground. Their multi-point analysis led to the conclusion that a Substorm Current Wedge (SCW) FAC system was driven by the BBFs observed in the inner magnetosphere and causing intense dB/dt fluctuations on the ground.

2.1.2 Prediction of soft proton intensities using machine learning

Kronberg et al. (2021) reported a unique analysis on the spatial distribution in the magnetosphere of energetic protons with energies from 28 to 962 keV, between 6 and 22 R_E. These protons are important as spacecraft with X-ray telescopes[2] can suffer from the impact of these protons as background, the so-called soft proton contamination. To tackle this problem, over 17 years of Cluster measurements, combined with machine learning techniques, now help to predict the intensities of these soft protons, showing improvements of up to 80% over previous techniques. The machine learning based model using Cluster data provides vital information for assessing particle contamination of X-ray telescopes, with regard to orbit and solar wind conditions. To enable reproducibility of their results and foster collaboration, the code data and weights of the trained models were made available via GitHub.[3]

2.2 Multi-scale plasma physics

Nakamura et al. (2021) present a unique conjugate observation of fast flows and associated current sheet disturbances in the near-Earth magnetotail, by MMS and Cluster preceding a magnetic substorm. More precisely, on September 8, 2018, these two missions detected, in the near-Earth magnetotail, a dipolarisation front (DF), while being around 4 R_E apart in the dawn–dusk direction. Similar electron acceleration signatures in the energy spectrograms revealed that both missions crossed the same DF. Thanks to these almost simultaneous ion scale and electron scale multi-point observations, 3D development of localised fast flows and current sheet disturbances caused by this DF, and preceding the development of a SCW, is presented in detail for first time.

2.3 Auroral plasma physics and citizen science

Northern lights are a fascinating natural phenomenon that have intrigued humankind for centuries. It is a naked eye observable phenomenon with various shapes and colours from auroral arcs that can last for hours to complex and more evanescent shapes like spiral aurora. Maetschke et al. (2023) have investigated auroral spiral pictures taken by a scientist attending a Cluster workshop in Tromsø, Norway, back in 2013 (see Fig. 1). For this, they combined space data from Cluster and THEMIS with pictures as a 'ground-based data set'. Complementary observations from Cluster and THEMIS, located up to 15 R_E on the nightside of Earth, suggest that the spiral may have been generated by an associated vortex in the magnetotail and then mapped along the magnetic field lines to the ionosphere, during a magnetic substorm.

It is worth noting that due to the paucity of data from all sky imagers (ASI) in the European Sector, this phenomenon was not captured by any ASI. On the positive side, it shows the potential for further studies using citizen science. It echoes other phenomena like STEVE originally found by citizen scientists/aurora photographers and characterised by Swarm measurements in situ (MacDonald et al. 2018). An ISSI (International Space Science Institute) working group is actively working on this subject and entitled: Auroral Research Coordination, Towards Internationalised Citizen Science (ARCTICS[4]).

[2] e.g., the ESA X-ray Multi-Mirror (XMM) mission or upcoming missions like the ESA/Chinese Academy of Sciences (CAS) Solar wind Magnetosphere Ionosphere Link Explorer (SMILE) or ESA New Advanced Telescope for High ENergy Astrophysics (ATHENA).

[3] https://github.com/Tanveer81/deep_horizon.

[4] https://collab.issibern.ch/arctics/.

Fig. 1 Temporal development of an auroral spiral, pictures taken in Tromsø in 2013 (credit: E.A. Kronberg, Munich University, Germany)

This result is also a particularly good preparation to the SMILE ESA/CAS mission that will specifically study auroras and is planned to be launched in 2025 or 2026.

2.4 Unexpected results related to lunar and Martian science

2.4.1 Evidence for lunar tide effects in Earth's plasmasphere

Everybody knows that Earth's ocean tides are induced by the Moon. What is less known is that these tides also impact the Earth's crust, the ionosphere, and the geomagnetic field near the ground (see Xiao et al. 2023 and references therein). More generally, tides are ubiquitous phenomena impacting spatially distributed systems, up to galactic scales (e.g. Renaud et al. 2009), as long as gravitational gradients are significant. For the first time, Xiao et al. (2023) reveals that a tide effect due to the Moon is also observed in a region filled with plasma, called the plasmasphere. This region is a torus of cold and dense plasma co-rotating with Earth from roughly 2 to 7 R_E.

To find this effect, they first derived the position of the outer boundary of the plasmasphere, called plasmapause, observed by multiple satellites over the past four decades, including the International Sun–Earth Explorer-1 (ISEE 1), Dynamics Explorer 1 (DE-1), Akebono, the Combined Release and Radiation Effects Satellite (CRRES), Polar, the Imager for Magnetopause-to-Aurora Global Exploration (IMAGE), Cluster, THEMIS and the Van Allen Probes. This work enabled to build a database of more than 50,000 plasmapause locations, or Lpp, spread across all Magnetic Local Time (MLT) sectors (Zhang et al. 2017). An example of how such plasmapause location can be derived is presented in Fig. 2a where an AC electric field spectrogram from 2 to 80 kHz measured by the Waves of High Frequency and Sounder for Probing of Density by Relaxation (WHISPER) experiment on Cluster 4 is displayed. In this figure, the inbound and outbound locations of the plasmapause, crossed by Cluster 4, is highlighted by black vertical dashed lines along sharp gradients of a light blue emission, corresponding to the upper hybrid wave signature.

Xiao et al. (2023) selected a subset of around 35,000 plasmapause locations, measured during low geomagnetic activity. A lunar tidal effect on the Lpp is shown in Fig. 2b, where Lpp perturbations as a function of MLT are presented for lunar position at 0 (full Moon), 6, 12 and 18 MLT. These panels reveal that the high tide peaks of the perturbations (see red dashed lines) progress regularly with lunar phase, and the high tide MLT is around 6 h ahead of the lunar phase.

This effect may be applicable to at least two additional planetary magnetospheres within our solar system, as well as exoplanet magnetospheres.

2.4.2 Properties of flapping current sheet of the Martian magnetotail

A planetary magnetotail current sheet is far from static: it oscillates, in part due to the fluctuating solar wind dynamic pressure, and twists in response to the interplanetary magnetic field (IMF). The properties of the flapping current sheet of the Earth's magnetotail have been studied in detail by Cluster and THEMIS including its amplitude, wavelength, and propagation speed (e.g. Zhang et al. 2002; Sergeev et al. 2003, 2004; Gabrielse et al. 2008). Zhang et al. (2023) presents the derivation of these flapping motion properties, but this time, for the Mars' induced magnetotail current sheet, based on NASA Mars Atmosphere and Volatile EvolutioN (MAVEN) data (see Fig. 3). These properties are then compared to Earth's flapping current sheet properties. Their analysis shows that the Martian magnetotail oscillations are 13 times more effective than on Earth to release the magnetic field energy of the induced magnetotail, hence playing a non-negligible role in the Martian magnetotail dynamics.

3 Scientific objectives (2021–2024)

The Cluster mission was originally planned to operate for two years. Thanks to its scientific productivity and the ingenuity of the Cluster flight control and flight dynamics teams at the European Space Operations Centre (ESOC), the Cluster mission was extended multiple times until this day (Escoubet et al. 2021). We present here the scientific objectives that have guided the operations

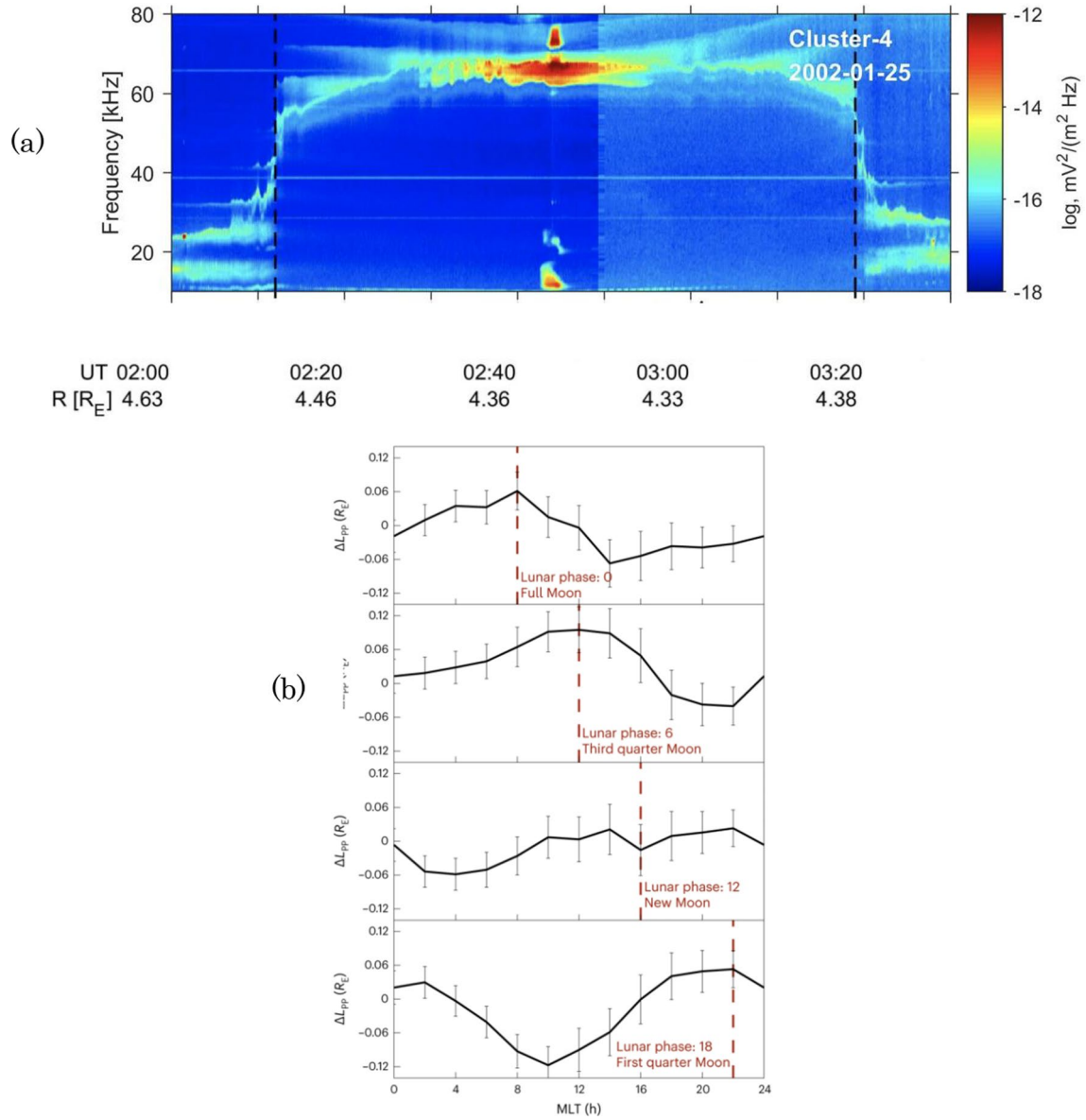

Fig. 2 **a** Electric field spectrogram from 2 to 80 kHz by the WHISPER instrument on C4, on 25 January 2002 from 02:00 to 03:40 UT; **b** variations of L_{pp} as a function of MLT for lunar phase at 0, 6, 12 and 18 MLT. Adapted from Xiao et al. (2023)

of the Cluster satellites since 2021. All 85 constellations manoeuvres performed since the beginning of the mission are shown in Fig. 4. As usual, there is always a delay between the operations, the calibration of the data and their exploitation by the scientific community. Hence, the full science exploitation of these data is yet to come. But as we will see, this is a treasure trove to exploit.

3.1 2021–2022 scientific objectives

In a nutshell, the 2021–2022 scientific objectives were focused on the following phenomena or regions:

- Southern and Northern cusp asymmetries.
- Magnetopause at electron, ion, and global scales.
- Extent of high-speed plasma jets in the magnetosheath.
- Plasmaspheric hiss origin.

3.1.1 Southern and Northern cusp asymmetries

The polar cusps are the polar regions in the Earth's magnetic field that are open to solar wind access. Since the entry of plasma and energy in the magnetosphere is

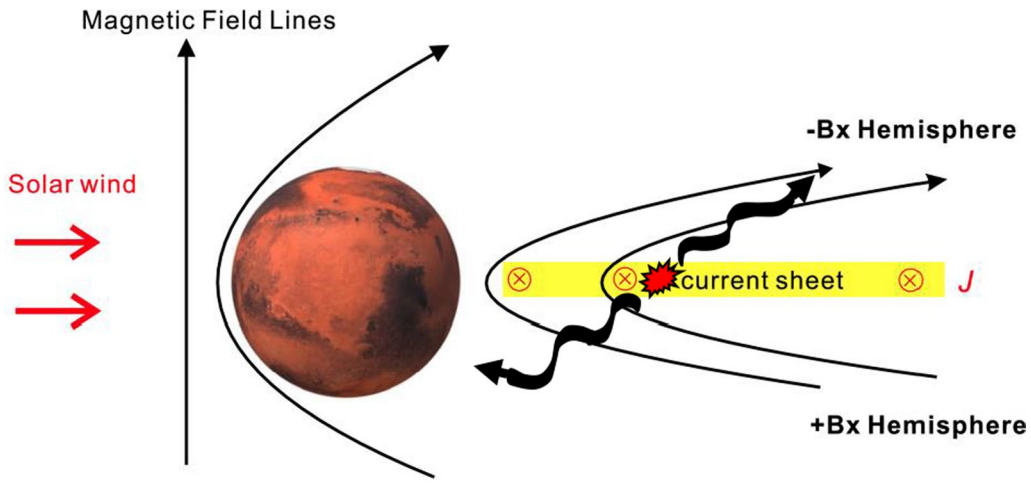

Fig. 3 Artistic illustration of the current sheet oscillations in the Mars' induced magnetotail. Adapted from Zhang et al. (2023)

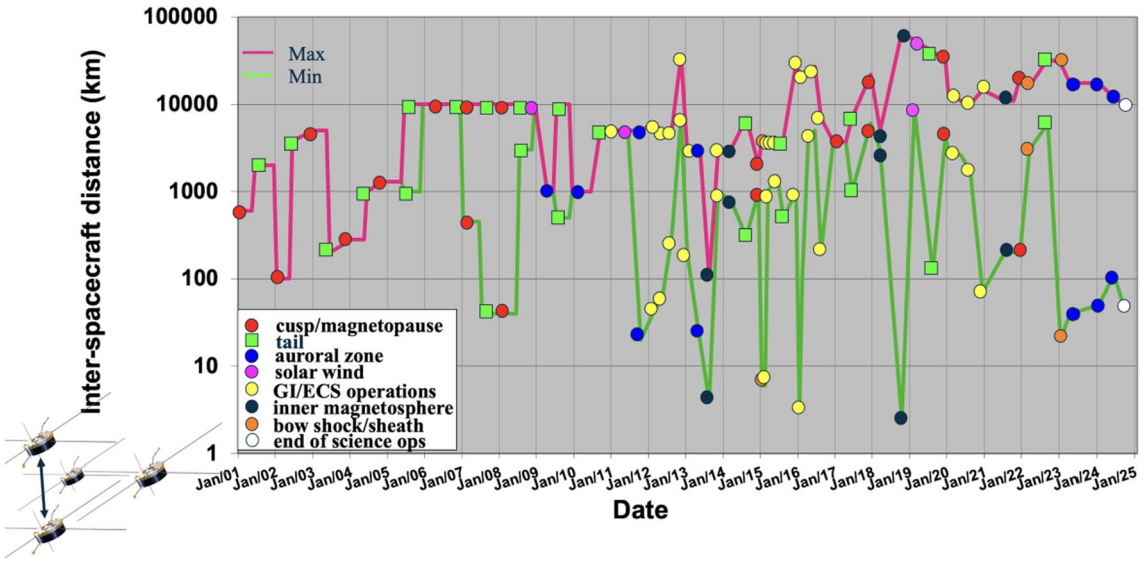

Fig. 4 Inter-spacecraft distance between the Cluster spacecraft from the beginning to the end of the mission. After 2005, the configuration of the constellation was not kept as a perfect tetrahedron during some periods of the orbit but instead, was configured to allow multi-scale measurements with Cluster 3 and Cluster 4 spacecraft separations down to a few kilometres at the bow shock in early 2015 (e.g. Dimmock et al. 2019); note that GI/ECS operations stands for Guest Investigator/Early Career Scientist (Escoubet et al. 2021)

essential to understand its dynamics, the polar cusp is therefore a key region that has been investigated since the early 1970s. Many measurements have been performed since then by polar orbiting satellites, but the multi-point measurements could only be started with Cluster (see review by Paschmann et al. 2005). Many properties of the polar cusp were then studied such as its motion following changes in the solar wind, its plasma properties and wave activity.

Since one cusp is present in each hemisphere, its North–South asymmetry has also been scrutinised. For instance, Newell et al. (1988) showed that the cusp was twice as large in summer as compared to winter and the electron and ion flux was 50% more intense in summer.

Figure 5 shows a sketch of the magnetosphere in winter in the Northern hemisphere (summer in the southern hemisphere) and two crossings of the cusp by the Defense Meteorological Satellite Program (DMSP) spacecraft. The cusp in winter (top right panel) is narrow (about 40 s) and presents low flux of electrons and ions (yellow regions in the centre of the plot). About 55 min later, the spacecraft crossed the summer cusp in the south hemisphere

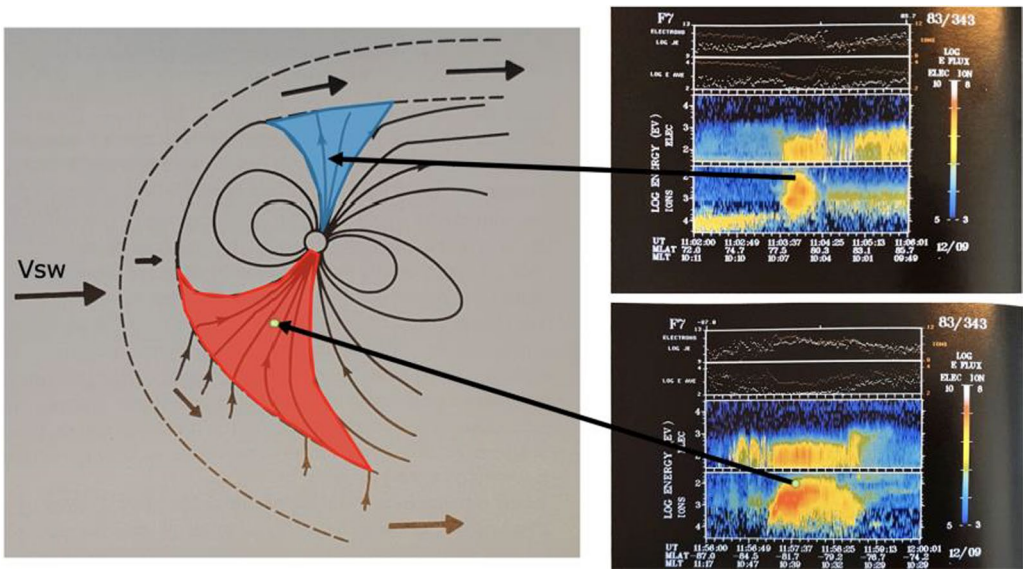

Fig. 5 Left: the magnetosphere in winter. The Northern and Southern cusp are sketched in blue and red, respectively. Top right: DMSP satellite crossing of the cusp in the Northern hemisphere on 9 Dec 1983 at 11:04 UT (the four panels from top to bottom are ion and electron energy flux, ion and electron average energy, electron energy–time spectrogram and ion energy–time spectrogram) Bottom right: DMSP satellite crossing of the cusp in the Southern hemisphere on 9 Dec 1983 at 11:57 UT. Adapted from Newell et al. 1988

(bottom right panel) and detected a stronger flux of ions and electrons (orange/yellow areas) lasting about 90 s. Newell et al. (1988) explained this as an effect of reconnection between the solar wind and the magnetosphere magnetic field lines as sketched on the left panel of Fig. 5.

Although statistical analysis confirmed this conclusion, one assumption in such study is that the solar wind conditions do not change between the winter and summer cusp crossings. The northern cusp crossing was separated by 55 min from the southern cusp crossing, which is a long time for the solar wind conditions to stay constant; solar wind conditions are usually varying on time scales of minutes to tens of minutes.

Another type of cusp asymmetry found with ground-based radar concerned Flux Transfer Events (FTEs). FTEs are created by reconnection at the magnetopause and have been first observed as bipolar signatures of the magnetic field at the magnetopause (Russell and Elphic 1978). They are solar wind magnetic flux tubes connected to the Earth's magnetic field. FTEs are usually expected to have connection in both the Northern and Southern hemisphere (e.g. Southwood et al. 1988). Unexpectedly, Milan and Lester (2001) found them in the Northern hemisphere cusp but not in the Southern hemisphere cusp, using incoherent scatter radar signatures.

To verify such cusp asymmetries, satellites would need to be crossing both the Northern and Southern cusp simultaneously. Fazakerley et al. (2005) presented a case study where Double Star TC-2 crossed the Northern mantle region (poleward of the cusp) while the Cluster spacecraft were crossing the Southern cusp. However, it was difficult to directly investigate cusp asymmetries since the mantle and cusp are different regions.

For the first time, simultaneous satellites observations of both cusps have been performed in 2021. The Cluster spacecraft have been crossing the northern cusp while the MMS spacecraft were crossing the southern cusp simultaneously (Fig. 6). This conjunction occurred

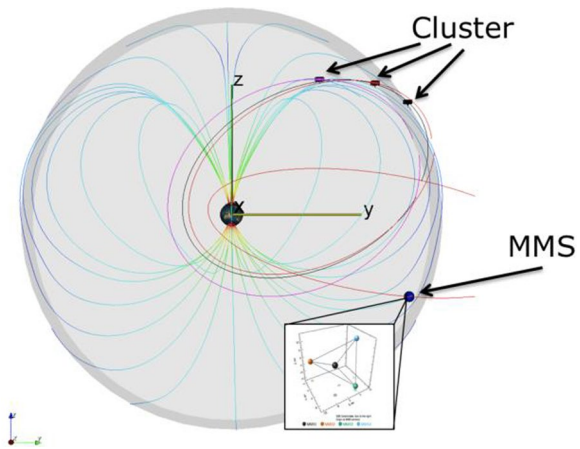

Fig. 6 Cluster orbit with a model of magnetosphere (green lines). Cluster spacecraft were crossing the northern hemisphere cusp and MMS the southern cusp simultaneously in November 2021. Pictures made with the Orbit Visualization Tool (https://ovt.irfu.se)

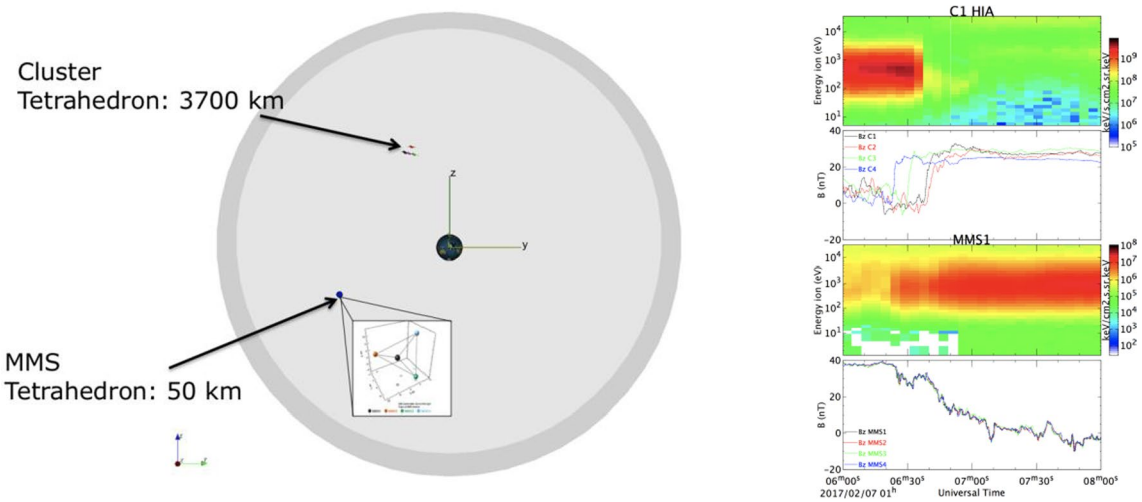

Fig. 7 Left part of the figure: magnetopause crossing with Cluster and MMS on 7 February 2017 in GSM coordinate system. Cluster tetrahedron size was 3700 km and MMS tetrahedron size was 50 km. Right part: Cluster 1 ion spectrogram and local B_z component of magnetic field from Cluster 1–4 (1st and 2nd panels). MMS 1 ion spectrogram and local B_z from MMS 1–4 (3rd and 4th panels) on 7 February 2017 (adapted from Escoubet et al. 2020)

in the northern hemisphere during winter. Thus, it is now possible to compare data acquired simultaneously in the Northern hemisphere cusp during winter with data acquired in the Southern hemisphere cusp during summer. FTEs occurrence will also be investigated with Cluster at multi-scales (ion and fluid) and MMS at electron scale making the two measurements highly complementary.

Additional North–South asymmetries are expected in the cusp location and plasma injection properties in response to the solar wind and IMF variations. Previously, it was shown that the cusp region moves from the local noon to opposite directions (towards dawn and dusk) in the different hemispheres in response to a particular orientation of the IMF. However, this research was based on a statistical analysis of cusp measurements in either the Northern or the Southern hemispheres. Investigation of the cusps formation during northward IMF orientation will also significantly benefit from simultaneous cusp observations in both hemispheres. These observations shall indeed allow to clearly distinguish between different mechanisms responsible for the formation of the cusps.

3.1.2 Magnetopause at electron, ion, and global scales

The left part of Fig. 7 shows a magnetopause crossing on 7 February 2017. Cluster was crossing the magnetopause at mid-latitude in the northern hemisphere with a tetrahedron size of 3700 km. MMS crossed the magnetopause in the Southern hemisphere on the dawn side with a tetrahedron size of 50 km. The separation of Cluster-MMS was [0.9, 4.56, 9.41] R_E. The right part of Fig. 7 shows the ion and magnetometer data from Cluster and MMS. The magnetopause is the sharp boundary seen on Cluster with the abrupt decrease of ion flux (red to green on 1st panel) and the sharp change in B_z component from near 0 nT in the magnetosheath to values above 20 nT in the magnetosphere. On the other hand, the MMS magnetopause crossing was extended over more than 1 min between 01:06:24 UT to 01:07:42 UT. The four MMS spacecraft being at 50 km from each other show very similar magnetic profiles (four lines superimposed in the bottom panel). The magnetopause speed and normal can be estimated from the four-spacecraft timing analysis. It gives a magnetopause moving outward at Cluster with a speed of 140 km/s and moving inward at MMS with a speed of 80 km/s. According to all magnetopause models, the magnetopause is expected to move in the same direction globally, however in this case the motion is different at two points separated by about 10 R_E. The global magnetopause models would need to be revised to consider such observation.

To confirm that such case is not a rare event, more conjunctions are needed where the time of magnetopause crossings is within a few minutes. Four more events in 2019–2020 and 21 more events were collected in 2021–2022. The large increase in 2021–2022 is due to a better orbital alignment of Cluster, MMS and THEMIS in 2022, hence forming a unique constellation of constellations (Fig. 8).

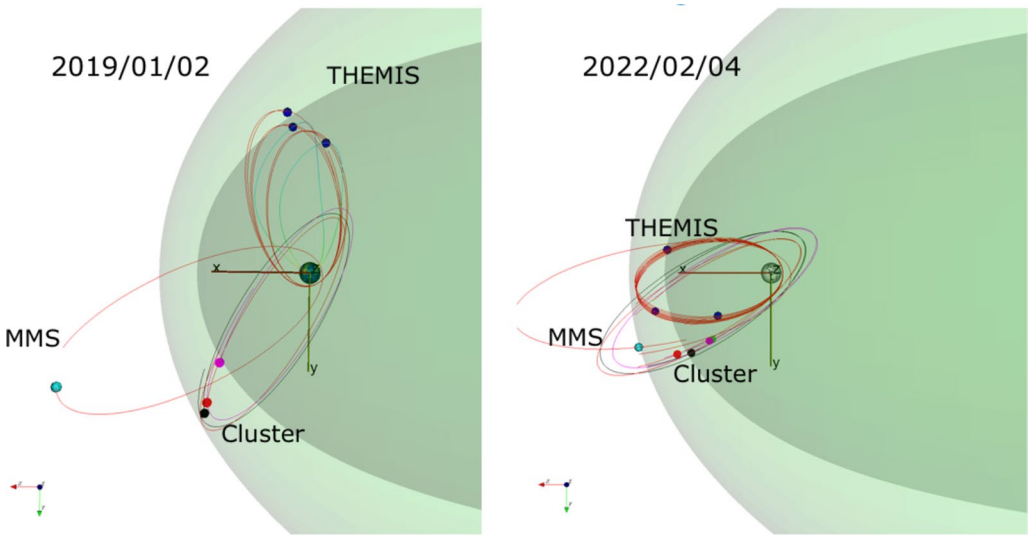

Fig. 8 Cluster, MMS and THEMIS orbits on 2 January 2019 (left) and 4 February 2022 (right). In 2022, their orbits were better aligned. The bow shock is the limit of the light green area (Farris et al. 1991 and Cairns et al. 1995) and the magnetopause the limit of the dark green area (Shue et al. 1997)

3.1.3 Extent of high-speed plasma jets in the magnetosheath

The Earth's magnetic field is an obstacle to the continuous flow of solar wind particles. Since this flow is supersonic, a bow shock is formed in front of the Earth's magnetic field and the solar wind is decelerated and heated. Sometimes, however, downstream of the shock, on its way toward the magnetosphere, high-speed jets (HSJs) are observed in ion data as if the solar wind was not decelerated (Nemecek et al. 1998; Savin et al. 2008; Amata et al. 2011). Hietala et al. (2009) first showed, using the four Cluster spacecraft, that these jets could be produced by ripples on the bow shock. Other explanations were proposed, such as discontinuities in the solar wind and ionised dust clouds carried by the solar wind. Since then, many studies have been performed to characterise HSJs (e.g. Archer and Horbury 2013; Plaschke et al. 2013).

However, one unsolved question remains: their extent over the dayside of the magnetosphere. It is an important aspect since the wider the dayside extent of HSJs is, the more deformation of the magnetosphere would be expected. Since these deformations may create ultra-low frequency waves, we may expect more energetic electrons in the radiation belts. The limited number of satellites was the main obstacle to address this problem. However, in 2022, Cluster, MMS and THEMIS covered a broad range of magnetic local time (Fig. 9) and collected data to address this question.

3.1.4 Plasmaspheric hiss origin

Baker et al. (2014) reported that 2–8 MeV energetic electrons in the radiation belts cannot penetrate closer than a geocentric distance r = 2.8 R_E (or 11,000 km of altitude). In other words, there seems to be an almost impenetrable barrier where these most energetic Van Allen belt electrons could not get closer to Earth. Although not fully understood, natural electromagnetic emissions in the inner magnetosphere could play a role. This is an important topic of research since such energetic electrons can create spacecraft anomalies or even destroy vital spacecraft electronic components. It is also important to understand and be able to predict the location of these energetic electrons for smooth operation of the continuously growing number of spacecraft in Medium Earth Orbit (MEO).

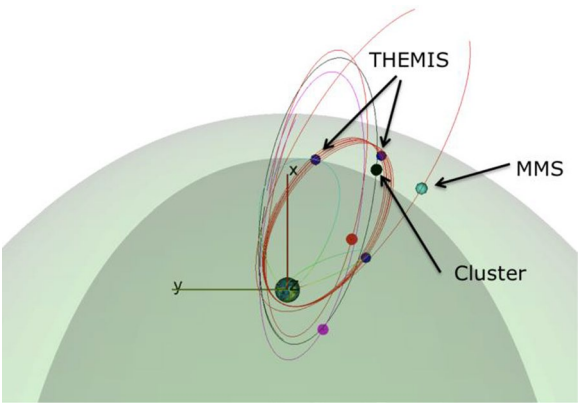

Fig. 9 Cluster, MMS and THEMIS orbits in March 2022. Please note the spread of the spacecraft in the magnetosheath, along the magnetopause (limit of the dark green area symbolising the magnetosphere)

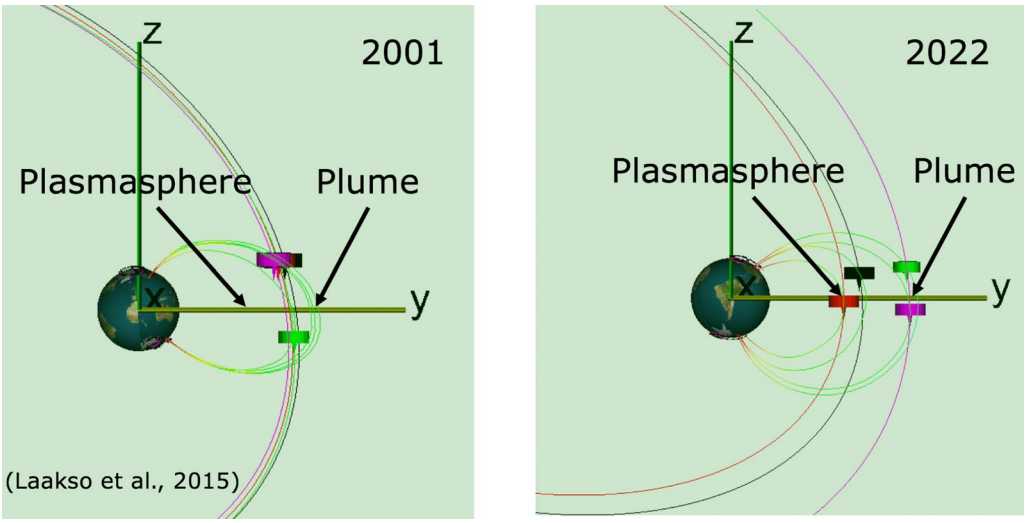

Fig. 10 Cluster orbits near perigee in 2001 from Laakso et al. (2015) and 2022 (right panel)

Plasmaspheric hiss (Thorne et al. 1973) is a natural electromagnetic emission at very low frequency (100 Hz–3 kHz). Its name is derived from its incoherent, structureless spectral properties which, when played through an audio system, sounds like white noise. Hiss has been measured on spacecraft since the late 1960s and, although many processes have been proposed to explain the generation of hiss, up to the mid 2000s, two main processes were generally accepted. The first one is the amplification of whistler mode waves by unstable energetic electron populations (Thorne et al. 1973; Cornilleau et al. 1985). The second one considers terrestrial lightning as the embryonic source to produce electromagnetic waves, which can then propagate to the plasmasphere (Sonwalkar and Inan 1989; Green et al. 2005).

In view of the difficulties to account for all hiss properties, Chum and Santolík (2005) proposed a third mechanism by which chorus waves, another type of natural electromagnetic waves, observed further away from Earth, would evolve into hiss after reflecting or refracting into the plasmasphere. Given that such a process would account to many hiss properties, Bortnik et al. (2008) presenting an analysis of a numerical simulation, suggesting that the chorus waves were the dominant source of plasmaspheric hiss.

Laakso et al. (2015) could pinpoint a source of hiss in a plasmaspheric plume, an elongated bulge-structure of the plasmasphere, where cold ionospheric and plasmaspheric plasmas drift towards the dayside magnetopause on the dusk side of the magnetosphere. The hiss waves were observed coming from the equatorial plume region, later bouncing back from the topside ionosphere as these waves were later detected propagating towards the equator in the inner plasmasphere in both the northern and southern hemispheres. This study shows that these frequently observed plumes could be an important source of hiss. Although no chorus waves were observed during these events, it does not preclude their contribution to hiss. Note however that the chorus is predominantly observed in the dawn sector.

In the events presented by Laakso et al. (2015), three spacecraft (C1, C2 and C4) were close to each other while the last one C3 was further away, allowing to investigate the two hemispheres at the same time (see left panel of Fig. 10). With approximately the same perigee altitudes, however, the plume and the plasmasphere could not be observed at the same time. In 2022, the orbits of the individual spacecraft changed significantly and their separations at perigee were around 1–2 R_E in altitude (see right panel of Fig. 10). This allowed to sample, for the first time, the plume and the plasmasphere simultaneously. In addition, the spacecraft along the orbit were moved such that two spacecraft were on each side of the equator, both in the plume and in the plasmasphere (see right panel of Fig. 10). This configuration of the Cluster spacecraft constellation enabled measuring the full path of hiss from the plume to the ionosphere and then the plasmasphere. In other words, this spacecraft constellation was ideally positioned to unambiguously find the source of plasmaspheric hiss.

3.2 January 2023–September 2024 scientific objectives

The two main scientific objectives for this period were the study of the (i) magnetospheric boundaries as part of a Geospace observatory; (ii) the Auroral Acceleration Region or AAR at high and low altitude sampling.

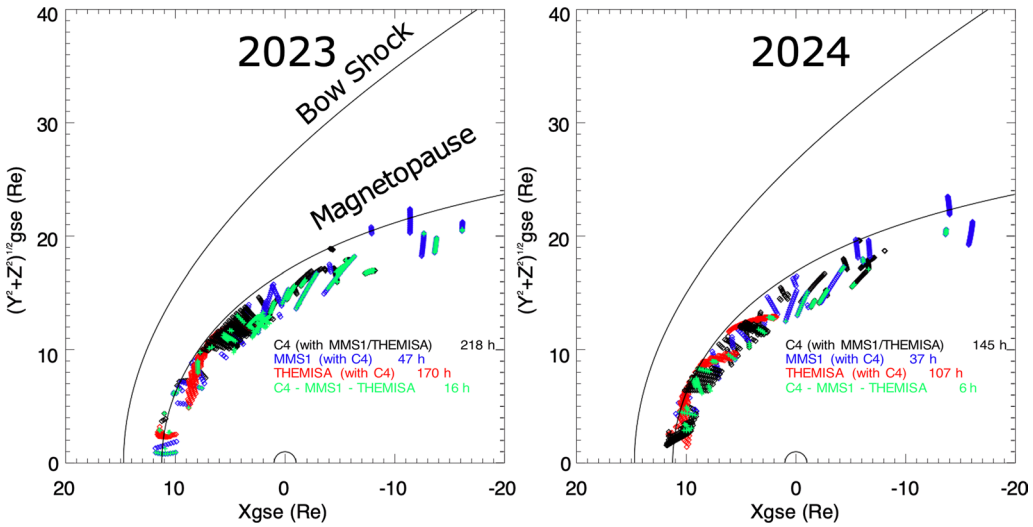

Fig. 11 Conjunctions between Cluster, THEMIS, and MMS at the magnetopause in 2023 and 2024

The first theme was a continuity of conjunctions with MMS and THEMIS planned in previous years. Along its roughly 50 h long orbit around Earth, Cluster experiments operate all the time in normal mode, except during around 4 h when they operate at higher time cadence or burst mode. As we will see, these conjunctions are relatively rare and require careful planning with modelled bow shock and magnetopause location to successfully achieve operating Cluster in burst mode during these time periods. Conjunctions with other missions are calculated using the NASA Space Physics Data Facility (SPDF)-Satellite Situation Center (SSC) web system, that contains the past and future orbit data from all heliophysics missions.

3.2.1 Magnetospheric boundaries as part of a geospace observatory

Observations of magnetospheric boundaries (magnetopause and bow shock) are key in understanding the energy flow and partition in plasmas (e.g. Rae et al. 2022). Cluster as part of the geospace observatory, including in particular THEMIS and MMS, provides a key component of these investigations. The uniqueness of Cluster is partly due to its near polar orbit, allowing measurements at high latitudes, contrary to THEMIS and MMS both orbiting near the equatorial plan.

Figure 11 displays all conjunctions in 2023 and 2024 at the magnetopause between Cluster, MMS, and THEMIS, using Cluster 4, MMS 1, and THEMIS-A as reference spacecraft. A double (or triple) conjunction is defined as follows: when two (or three) of these reference spacecraft are located at the Roelof and Sibeck (1993) magnetopause model ± 1 R_E. For the whole year of 2023, double conjunctions were found to occur during 218 h at/near the magnetopause while triple conjunctions occurred for 16 h. For 2024 (whole year), these conjunctions drop a bit to 145 h for double and 6 h for triple conjunctions.

Figure 12 presents the conjunctions at the bow shock. This time, a double (or triple) conjunction is defined as follows: when two (or three) of these reference spacecraft are at the Fairfield (1971) bow shock model ± 2 R_E. For the whole year of 2023, double conjunctions occurred during 238 h at/near the bow shock and during 5 h for triple conjunctions. For 2024, these conjunctions increase a bit to 295 h for double and 21 h for triple conjunctions.

3.2.2 Auroral acceleration region at high and low altitude

Auroral plasma physics was not initially a primary objective of the nominal phase of the Cluster mission. However, the unique ability to estimate FAC and measure DC electric fields, energetic ions, and electrons above the AAR, revealed for the first time the temporal variation within a couple of minutes of auroral phenomena. This uniqueness is mainly due to four spacecraft orbiting the Earth, along very similar polar or inclined orbits, in a string of pearls configuration when crossing auroral field lines.

The first paper published in *Nature*, based on Cluster data, presented an analysis of such measurements during a black aurora, which enabled to derive a theory explaining for the first time this phenomenon (Marklund et al. 2001). Similar spatio-temporal analyses of other auroral phenomena followed (e.g. Marklund et al. 2004; Figueiredo et al. 2005).

The evolution of the Cluster orbit from its nominal polar orbit to an inclined orbit allowed unique

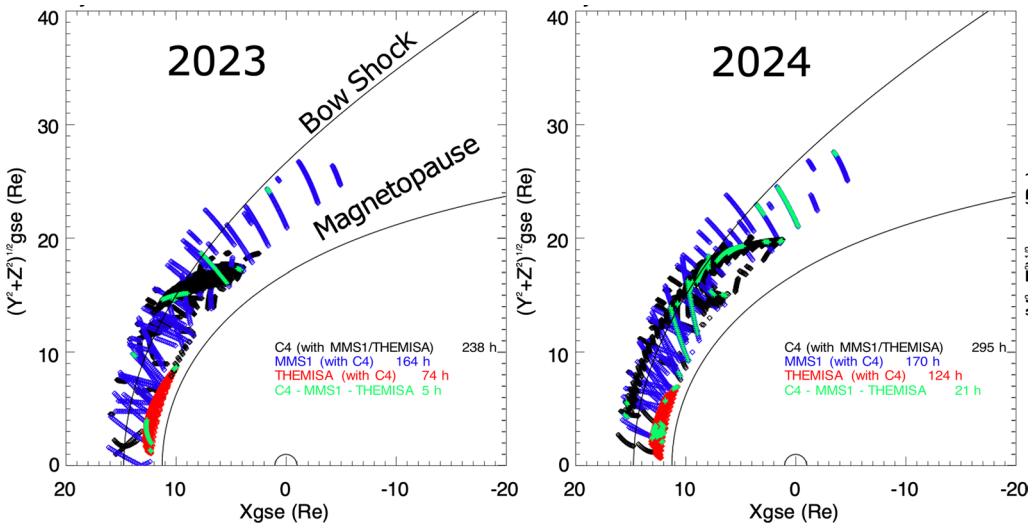

Fig. 12 Conjunctions between Cluster, THEMIS, and MMS at the bow shock in 2023 and 2024

measurements in the AAR, a first with multiple spacecraft. This occurred for the first time in 2009–2011, where burst mode was activated in the AAR with a special ground-based support by the NASA Deep Space Network for the high time resolution AC electric and magnetic wave instrument named WideBanD (WBD). This special data campaign led to numerous publications (e.g. Marklund et al. 2009; De Keyser et al. 2010).

However, at that time, the separation between the spacecraft was small and simultaneous sampling at different altitudes within the acceleration region was limited to separations in altitude of only a fraction of an Earth's radius, covering only part of the total acceleration voltage. Statistical studies combining multi-spacecraft Cluster observations, not taken simultaneously, were used to draw an average picture of the electric potential profile of the AAR (e.g. Alm et al. 2015a, 2015b). Although due to the orbit constraints, the full altitude range of interest (up to 6 R_E) was not covered, and simultaneous measurements were lacking at larger altitude separations.

During 2023 and the first few months of 2024, such measurements were obtained, because the perigee altitude decrease was much faster than in 2009–2011. Cluster 3 and 4 crossed the nightside auroral oval at altitudes of around 16,500 km, Cluster 1 at 10,200 km and Cluster 2 at 5700 km. Swarm was also crossing the nightside auroral zone in the same period and measured the ionospheric currents powering the aurora at 500 km (see Fig. 13).

4 Spacecraft re-entry: opportunities for science

From launch to re-entry, the ESA spacecraft are closely monitored by experts at ESOC, in concert with international private and public satellite operators. The re-entry of its spacecraft assets falls under the ESA Space Debris Mitigation Policy for Agency Projects (ESA 2023). As we will see, where appropriate, manoeuvres are planned to avoid the circularisation of their orbit, which could otherwise potentially lead to inert space debris. The re-entry itself is also carefully analysed to respect ESA Re-entry Safety Requirements (ESA 2017), especially avoiding any impact over populated areas.

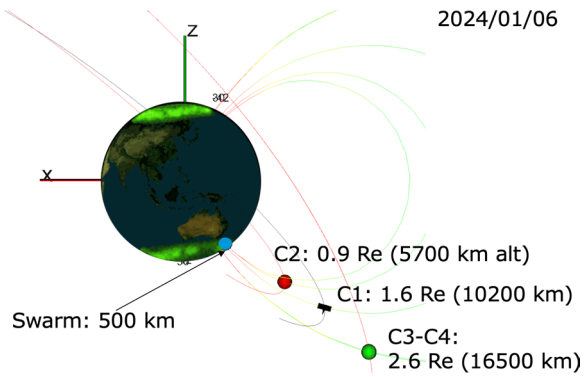

Fig. 13 Position of the four Cluster satellites and the Swarm constellation on 2014-01-06 covering the AAR at low and high altitude. The image of Earth's is illustrative, it is an image taken by NASA's Polar spacecraft (1996–2008)

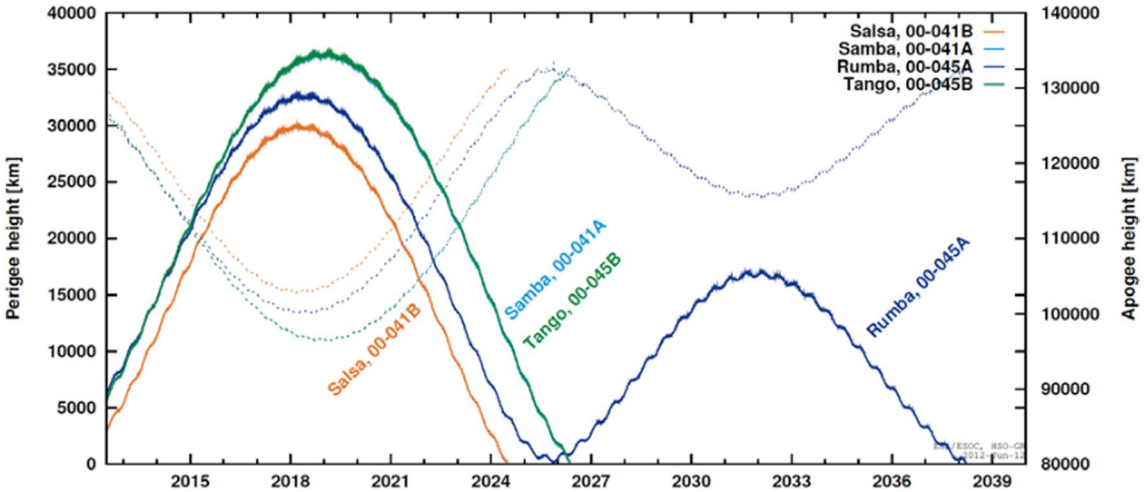

Fig. 14 Perigee of the orbit of C1 (Rumba), C2 (Salsa), C3 (Samba) and C4 (Tango) predicted in 2012

4.1 Re-entry latitude

As underlined in Sanvido (2023), for missions like Cluster flying in Highly Elliptical/Eccentric Orbit (HEO), the dominant perturbation of their orbits is due to the Moon and Sun gravity fields. These fields create a strong oscillatory variation of their orbital eccentricity value, resulting in an oscillation of their perigee altitude, while the orbital semimajor axis remains almost constant. The effect of the Sun gravitational field is six times stronger than the lunar field for the long-periodic oscillations, leading to a perigee altitude variation of the order of 200 km due to the Sun and few tens of kilometres due to the Moon. These effects are visible for the Cluster spacecraft in Fig. 14, which shows the temporal evolution of perigee (solid line) and apogee (dashed line) estimated in 2012.

During the last few perigee passes before re-entry, the combination of these effects may lead to two scenarios: either they compensate each other, translating to a slow decrease of the altitude and circularisation of the orbit, or they superimpose, leading to a steep re-entry with higher velocity and steep path angle. In the latter case, the atmospheric breakup of the satellites occurs near the location of their perigee. This behaviour can be exploited to potentially control the latitude band of the breakup process and the impact area for possible surviving fragments. After an in-depth mission analysis by ESA (e.g. Lemmens et al. 2016), a manoeuvre was performed early 2015 to lower the C1 (Rumba) orbital apogee to make it re-enter in 2025, with a perigee location in the southern hemisphere. This manoeuvre shortened the C1 re-entry by more than a decade with respect to the previous re-entry conditions, while the natural decay would have resulted in a re-entry over the northern hemisphere at latitudes with denser populated areas.

4.2 Re-entry longitude

The final re-entry point longitude analysis aims at a steep re-entry over oceans, minimising the risk of fragments impacting land (Sanvido 2023). Solar pressure and atmospheric drag play a major role in the final perigee evolution and longitude targeting, potentially leading to circularisation of the orbit and consequent longitudinal spreading of the footprint. Consequently, the longitude targeting of the suitable re-entry spots focuses both on researching re-entries over specific uninhabited areas (see grey areas in Fig. 15 bottom panel), and on identifying re-entry options that exclude the orbit circularisation during the last perigee passes (Fig. 15 top panel). Once a re-entry option satisfies these criteria, a final stochastic analysis is performed perturbing the re-entry orbit in order to obtain a robust prediction of the re-entry area against uncertainties.

4.3 Cluster 2 re-entry

In-depth analysis of the C2 orbit natural decay led to the conclusion that its orbit would circularise (ESA internal technical note, private communication). Different options of manoeuvres were investigated and the best option (option 3 in Fig. 15) was chosen. This option will enable a safe re-entry in the Pacific Ocean, west of Easter island, with a probability of only 1 in 10,000 to violate its exclusive economic zone area. Twenty-four fragments of the C2 spacecraft could potentially hit the water. The manoeuvre was successfully executed on 16 January 2024.

ESA re-entry safety requirements impose, in particular, that the re-entry of the space system, or elements thereof, shall not result in hazards to human population, harmful

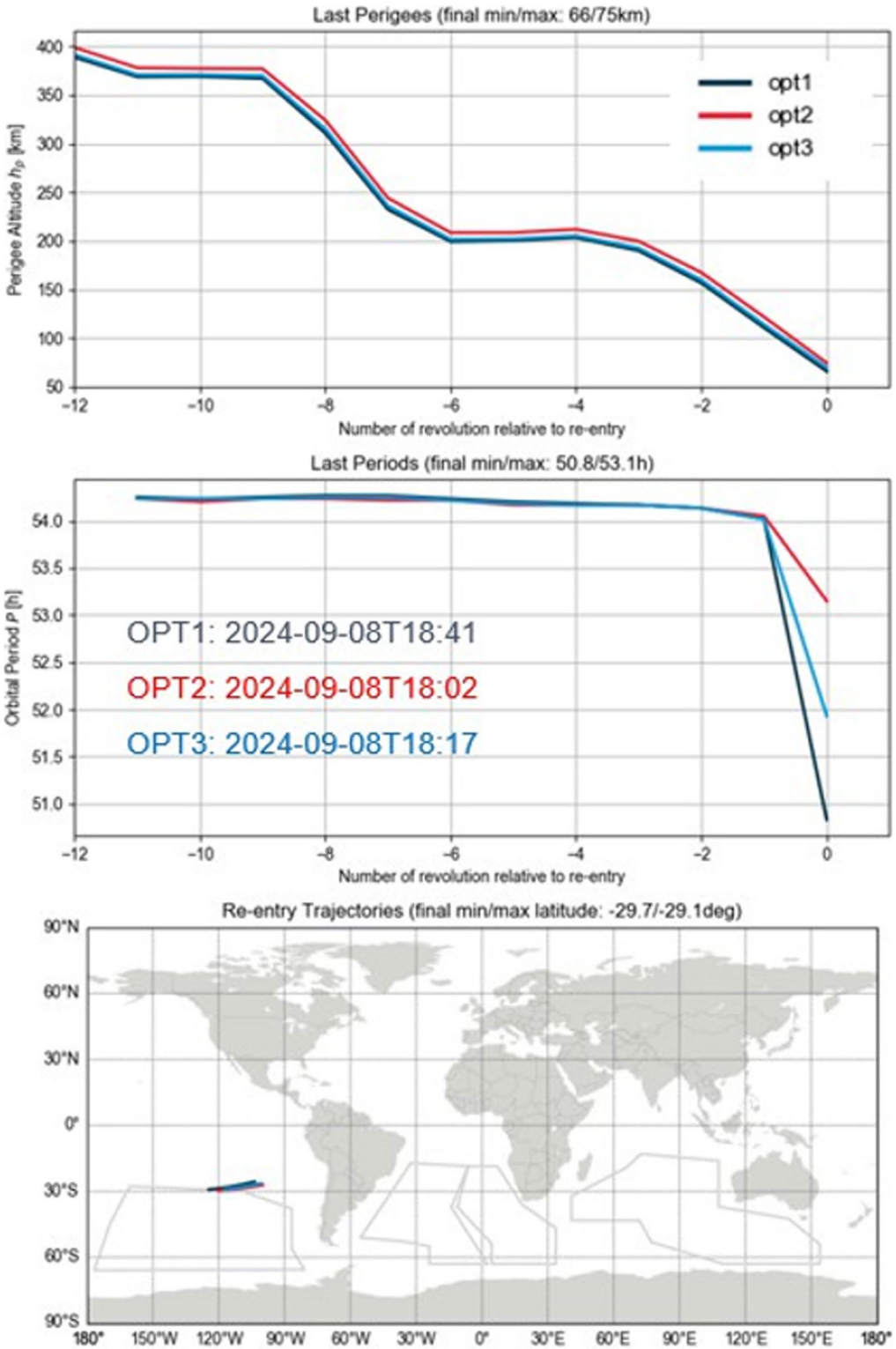

Fig. 15 Cluster 2 re-entry locations for three optimal re-entry options. The 3rd option was chosen

contamination of the Earth environment, nor damage to assets, due to:

- o Impacting fragments
- o Floating fragments
- o Pressurised or explosive fragments
- o Hazardous chemical substances
- o Radioactive substances

Simulations performed by Sanvido (2023) suggest that possible floating elements, like tanks, are not re-entering intact, and are expected to sink. Other ESA re-entry safety requirements are detailed in Appendix A while the full list of requirements can be found in ESA (2017). Similar final optimisations of the orbit of the three other Cluster satellites have been performed and necessary manoeuvres are now planned.

4.4 Scientific benefits of the Cluster spacecraft re-entries

On 8th September 2024, the Cluster 2 spacecraft will re-enter and burn up in the Earth's atmosphere. This re-entry and the follow-up re-entries in 2025 and 2026 will be a rare opportunity to observe the burn up of four identical spacecraft under different ionospheric conditions. The ESA space debris office will run dedicated observation campaigns to collect as much information as possible, to eventually improve its space debris re-entry models. An airborne campaign will be conducted, taking off from Easter Island. The airplane will be equipped with InfraRed (IR) camera and spectrometers. Spectroscopy will allow to distinguish the elements remaining during the re-entry, indicating which type of material (e.g. aluminium, steel) burn up first. These rare measurements may be difficult to capture and are not guaranteed, but if successful, will eventually help improve the ESA space debris models.

5 Preparing its legacy: complete archive and advanced tools

As underlined in Escoubet et al. (2021), the development of an open Cluster archive has enabled a boost in the scientific return of the mission. It has clearly widened its usage to scientists with lead authors of refereed publications from 43 countries, i.e. a worldwide impact. A bit more than half of the first authors of all 3200 + Cluster refereed papers are associated with laboratories from ESA member states, while 25% are related to US labs, 15% from China and 10% for the rest of the world.

The Cluster Science Archive (CSA) makes available an online Graphical User Interface at https://csa.esac.esa.int with capabilities to:

- search and download the best calibrated datasets and ancillary data,
- inspect the datasets' metadata,
- access quicklook plots,
- visualise pre-generated and on-demand time series, spectrograms, and distribution functions,
- browse through pre-generated and on-demand inventory plots,
- perform data mining.

This online capability is completed by a command line access using the International Virtual Observatory Alliance (IVOA) standard Table Access Protocol (TAP[5]), allowing to download directly up to 1 GB and asynchronously (up to 50 GB) or even stream data (useful for software applications). A couple of features are unique to CSA in terms of data and graphical products content. Here are some highlights.

The ancillary data contain key housekeeping engineering parameters measured onboard each Cluster satellite over 20 years, which is a treasure trove for engineering studies, and very rarely preserved in a systematic way especially with similar metadata as the datasets. Cross-calibration graphical plots have been systematically generated to allow the comparison of the same physical quantities (e.g. electron density, DC electric field, DC magnetic field) using different measurement techniques.

The CSA complies with international standards. While users can download data in its native ASCII Cluster Exchange Format (CEF), a data format converter has been developed in house to convert the data format on the fly to the Common Data Format (CDF) with metadata following the International Solar-Terrestrial Physics (ISTP) guidelines. A Heliophysics data Application Programming Interface or HAPI (Weigel et al. 2021) has been developed on top of the TAP server to make the data available easily in Python, MATLAB or IDL (https://hapi-server.org/servers/). The CSA has been working hand in hand with major Space Physics multi-missions' data analysis open-source software such as the Space Physics Environment Data Analysis Software or SPEDAS (Angelopoulos et al. 2019), Autoplot (Faden et al. 2010) or the IRFU-Matlab software.[6]

Three advanced tools have been recently developed by the ESA archive team and made publicly available (https://csa.esac.esa.int/csa-web/#tools): a data mining tool, an advanced interactive plotting tool and a Bryant plotting tool. For the data mining tool, 86 key physical and orbital parameters, at 1 min resolution have been

[5] Table Access Protocol: https://www.ivoa.net/documents/TAP/.

[6] IRFU-MATLAB software: https://github.com/irfu/irfu-matlab.

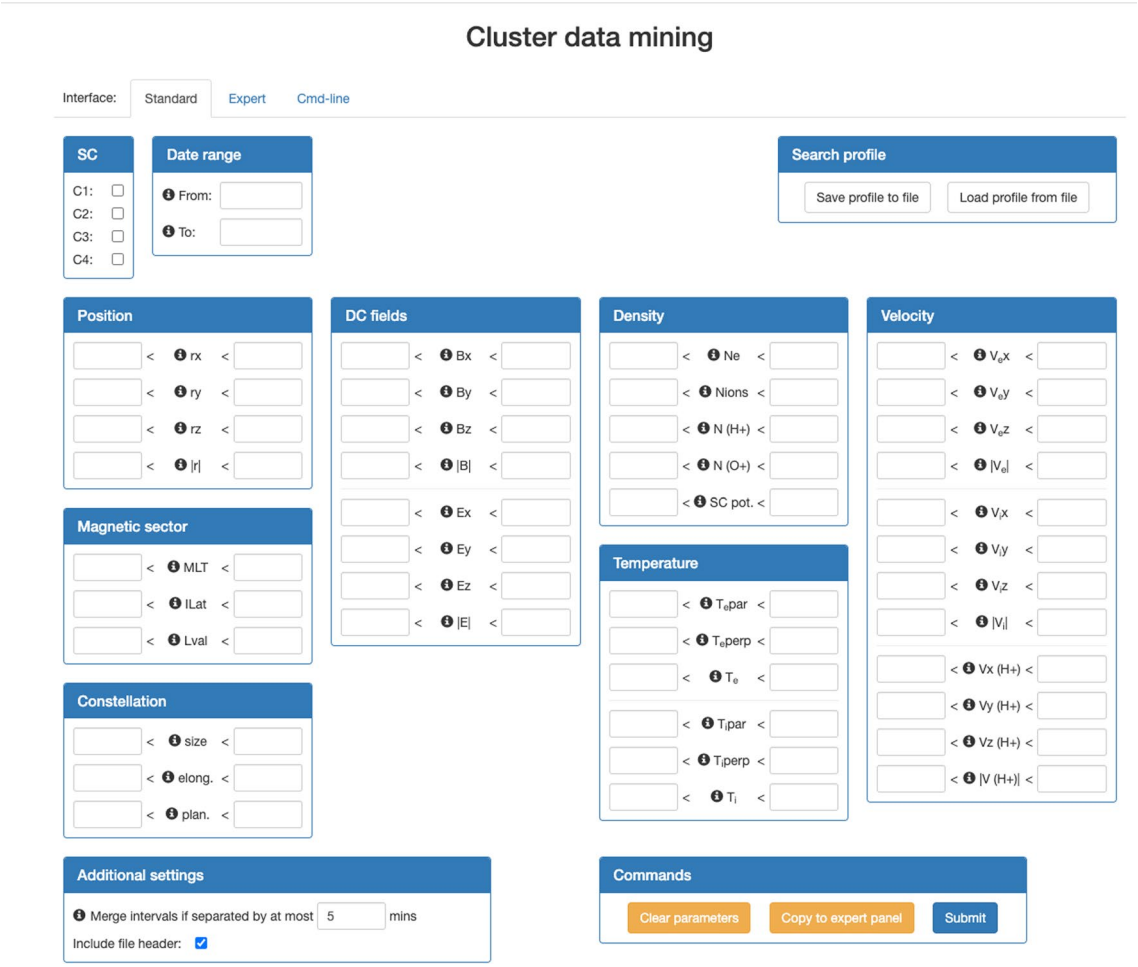

Fig. 16 The Cluster Science Archive data mining tool allowing to derive time periods from a particular region of space, physical conditions and even constellation configuration (https://csa.esac.esa.int/csa-web/#tools)

generated for the whole mission, for each spacecraft. This tool allows a user to search the time periods from a particular region of space, under a specific range of physical parameters and even for a specific elongation and planarity of the Cluster spacecraft constellation, without any knowledge of the name and functioning of the instruments onboard (see Fig. 16).

These averaged parameters are also available to download. The advanced interactive plotting tool allows fast online plotting of key physical parameters (high-resolution or averaged) with quality plots, directly insertable in refereed papers. The Bryant plotting plot displays an averaged physical parameter along orbits together with boundaries/regions markers. For instance, users can quickly generate one year of electron flux measured by Cluster 4, with the bow shock, magnetopause, and neutral sheet markers overplotted (see Fig. 17).

An on-going study, supported by ESA, will start delivering, in 2024, datasets identifying the various magnetospheric boundaries crossed by each Cluster satellite over the entire mission (e.g. bow shock, magnetopause, cusp, plasmasheet, plasmapause, etc.). These boundaries crossings datasets will be a key value-added product for the community, in particular for statistical studies. These datasets will be made available in the archive.

After the end of operations (30 September 2024), a 2-year post-operations period will start for the archive. The main goal is to complete its data content with data measured in 2023 and 2024. Almost none of the Cluster instruments can be calibrated in isolation but depend on each other (e.g. DC magnetic field necessary to derive parallel and perpendicular electron temperature), which requires time for all instruments to be fully calibrated. A data ingestion capability after the post-operations phase will remain available in case of a re-delivery of better calibrated versions of some datasets. Documentation, such as instruments' user guide and calibration report, shall be

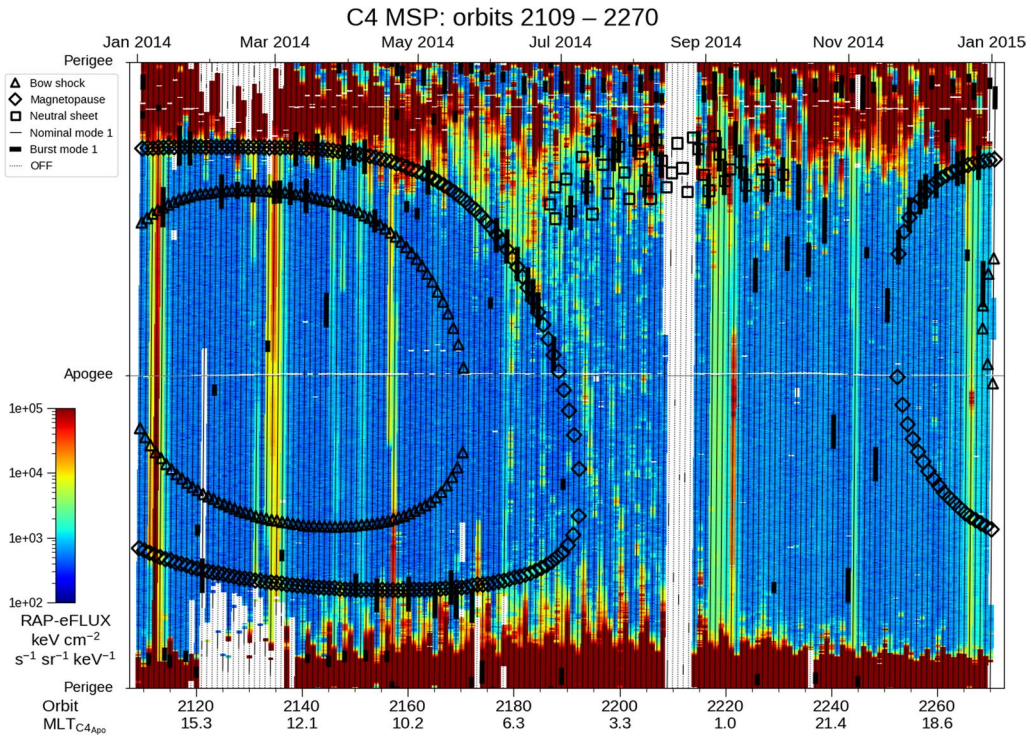

Fig. 17 Energetic electron fluxes at 1 min resolution measured by Cluster 4 in 2014, displayed along the orbits (in a so-called Bryant plot). Markers of the bow shock, magnetopause and neutral sheet are overplotted when crossed

fully updated and delivered. For long-term preservation, all documents will be directly ingested in the archive and made available together with the data. Eventually, the CSA itself will be integrated in a single multi-missions heliophysics archive.

6 Conclusion

Cluster is the first constellation of four scientific spacecraft to study the Earth–Sun connection in three dimensions. Cluster has been operating along with Geotail, THEMIS, Van Allen Probes, Swarm, MMS, Arase, constituting the Heliophysics/Geospace System Observatory by combining single satellite missions and constellations of 2, 3 and 4 spacecraft together. This is essential to study the effect of the Sun on the Earth environment, which through these observations has been revealed to be a varying and multi-scaled system of systems and has highlighted the need for more dedicated coordination of missions in the future (e.g. Kepko et al. 2024).

The four Cluster spacecraft were unique in their ability to obtain a three-dimensional picture of medium and large-scale plasma structures along a polar and then oblique orbit; MMS is focusing on small electron scale structures and THEMIS on fluid scales structures in the equatorial plan. The Cluster spacecraft formation varied in size naturally around the orbit, while 85 constellations manoeuvres were performed over the course of the mission. This has enabled unique multi-point measurements of different regions at different scales.

A key aspect of the new science investigations over the various extensions has been the orbit evolution due to Sun–Moon gravitational perturbations. This has drastically changed Cluster's nominal orbital parameters over time and facilitated access to regions of near-Earth space that were not originally targeted (e.g. the AAR).

An extensive overview of the scientific output, operations challenges and the data distribution and archiving efforts during the first 20 years of the Cluster mission is detailed in Escoubet et al. (2021).

We presented here, first, a quick summary of a few scientific highlights published since then. This subjective choice was guided by our intention to show the range of topics covered by this mission, including space weather science, multi-scale plasma physics, auroral plasma physics and citizen science, and its use in comparing magnetospheric phenomena between planets.

The latest scientific objectives, from 2021 to the end of its operations (September 2024), were then presented. During these years, the Cluster mission was operated to maximise the conjunctions occurring with other single and multi-spacecraft constellations to achieve system level magnetospheric science, impossible to achieve by a

single mission. We can only hope that this pioneer mission will be followed by future multi-spacecraft, multi-scale missions like Plasma Observatory (Retinò et al. 2022) and HelioSwarm (Klein et al. 2023), necessary to understand physical phenomena at electron, ion, and fluid scales simultaneously.

But end of operations does not mean end of science. The re-entry itself of each spacecraft is also an opportunity to collect unique measurements of the disintegration of the same satellite under different ionospheric conditions. This will eventually improve space debris models to better predict re-entry of satellites, which is of crucial importance for humankind.

Finally, the post-operations (2024–2026) and the legacy phase of the mission are there to complete the archive and make sure that this treasure trove of data is preserved for the upcoming decades by the ESAC Science Data Centre of the European Space Agency.

Appendix A

ESA re-entry safety requirements

ESA re-entry safety requirements imposes in particular that:

- The space system shall be designed and operated such that the re-entry casualty risk does not exceed 10^{-4} for all re-entry events.
- The re-entry of the space system, or elements thereof, shall not result in hazards to human population, harmful contamination of the Earth environment, and damages to assets, due to:
    - Impacting fragments,
    - Floating fragments,
    - Pressurised or explosive fragments,
    - Hazardous chemical substances,
    - Radioactive substances.
- The re-entry casualty risk shall include all the impacting fragments of the space system with a kinetic energy equal or greater than 15 Joules (J) at their impact on Earth surface.
- The operator of the space system shall keep an up-to-date record of the space system status demonstrating the ability of the space system and the availability of the energy resources to perform the de-orbit and re-entry manoeuvres to comply with the re-entry safety requirements.
- Retrieval operations shall be performed every time wrecks from a re-entered space system, or elements thereof, represent hazard to human health or Earth environment
- The retrieval options shall be executed in accordance with local national safety regulations and in agreement with local government authorities

The full extent of ESA Re-entry Safety Requirements is detailed in (ESA 2017).

Abbreviations

AAR	Auroral acceleration region
AC	Alternating current
ATHENA	Advanced Telescope for High ENergy Astrophysics
CDF	Common data format
CEF	Cluster exchange format
CSA	Cluster science archive
DC	Direct current
DF	Dipolarisation front
DMSP	Defense meteorological satellite program
ESDC	ESAC science data centre
ESOC	European Space Operations Centre
FAC	Field aligned current
GI/ECS	Guest investigator/early career scientist
GIC	Geomagnetically induced current
HAPI	Heliophysics data application programmer's interface
HEO	Highly elliptical orbit
HSJ	High-speed jets
IMF	Interplanetary magnetic field
IR	InfraRed
IVOA	International Virtual Observatory Alliance
ISTP	International solar terrestrial physics
MAVEN	Mars Atmosphere and Volatile EvolutioN
MEO	Medium earth orbit
MMS	Magnetospheric MultiScale
R_E	Earth radius
SCW	Substorm current wedge
SMILE	Solar Wind Magnetosphere Ionosphere Link Explorer
SPEDAS	Space Physics Environment Data Analysis Software
SSC	Satellite Situation Center
TAP	Table Access Protocol
THEMIS	Time history of events and macroscale interactions during substorms
WBD	WideBanD
XMM	X-ray multi-mirror

Acknowledgements

C.P. Escoubet thanks NASA SPDF-SSCweb system for making the orbits and models available to identify spacecraft conjunctions. The authors would like to thank all scientists and engineers who have made Cluster the success it is today. In particular, we remember those dear Cluster colleagues who are not able to share these final stages of this amazing mission.

Author contributions

The main authors of this paper are Arnaud Masson and C. Philippe Escoubet. Matthew G.G.T. Taylor, B. Sousa, B. Abascal Palacios, D. Sieg and S. Lemmens have reviewed the paper and provided valuable contribution to the original draft.

Funding

No specific funding declared.

Availability of data and materials

All Cluster data are public and available at https://csa.esac.esa.int. Output of ESA orbit simulations are not public data.

Declarations

Ethics approval and consent to participate

Not applicable.

Consent for publication
Not applicable.

Competing interests
All co-authors of this manuscript declare no financial and non-financial competing interests.

Author details
[1]European Space Agency, European Space Astronomy Center, Camino Bajo del Castillo, s/n Urbanización Villafranca del Castillo, Villanueva de la Cañada, 28692 Madrid, Spain. [2]European Space Agency, European Space Research and Technology Centre, Keplerlaan 1, 2201 AZ Noordwijk, The Netherlands. [3]European Space Agency, European Space Operations Centre, 5 Robert-Bosch Strasse, Darmstadt, Germany. [4]IMS Space Consulting for ESA, European Space Agency, European Space Operations Centre, 5 Robert-Bosch Strasse, Darmstadt, Germany. [5]LSE Space for ESA, European Space Agency, European Space Operations Centre, 5 Robert-Bosch Strasse, Darmstadt, Germany.

Received: 30 April 2024 Accepted: 18 August 2024
Published online: 30 August 2024

References

Alm L, Li B, Marklund GT, Karlsson T (2015a) Statistical altitude distribution of the auroral density cavity. J Geophys Res Space Phys. https://doi.org/10.1002/2014JA020691
Alm L, Marklund GT, Karlsson T (2015b) Electron density and parallel electric field distribution of the auroral density cavity. J Geophys Res Space Phys. https://doi.org/10.1002/2015JA021593
Amata E, Savin SP, Ambrosino D et al (2011) High kinetic energy density jets in the Earth's magnetosheath: a case study. Planet Space Sci 59:482–494. https://doi.org/10.1016/j.pss.2010.07.021
Angelopoulos V (2008) The THEMIS mission. Space Sci Rev 141:5–34. https://doi.org/10.1007/s11214-008-9336-1
Angelopoulos V, Cruce P, Drozdov A et al (2019) The Space Physics Environment Data Analysis System (SPEDAS). Space Sci Rev 215:9. https://doi.org/10.1007/s11214-018-0576-4
Archer MO, Horbury TS (2013) Magnetosheath dynamic pressure enhancements: occurrence and typical properties. Ann Geophys 31:319–331. https://doi.org/10.5194/angeo-31-319-2013
Baker D, Jaynes A, Hoxie V et al (2014) An impenetrable barrier to ultrarelativistic electrons in the Van Allen radiation belts. Nature 515:531–534. https://doi.org/10.1038/nature13956
Bolduc L (2002) J Atmos Solar Terr Phys 64(16):1793–1802. https://doi.org/10.1016/S1364-6826(02)00128-1
Bortnik J, Thorne RM, Meredith NP (2008) The unexpected origin of plasmaspheric hiss from discrete chorus emissions. Nature 452:62–66. https://doi.org/10.1038/nature06741
Boteler DH, Pirjola RJ, Nevanlinna H (1998) The effects of geomagnetic disturbances on electrical systems at the Earth's surface. Adv Space Res 22(1):17–27. https://doi.org/10.1016/S0273-1177(97)01096-X
Burch JL, Moore TE, Torbert RB, Giles BL (2016) Magnetospheric multiscale overview and science objectives. Space Sci Rev 199(1):5–21. https://doi.org/10.1007/s11214-015-0164-9
Cairns IH, Fairfield DH, Anderson RR et al (1995) Unusual locations of Earth's bow shock on September 24–25, 1987: Mach number effects. J Geophys Res 100:47–62. https://doi.org/10.1029/94JA01978
Chum J, Santolík O (2005) Propagation of whistler-mode chorus to low altitudes: divergent ray trajectories and ground accessibility. Ann Geophys 23(12):3727–3738. https://doi.org/10.5194/angeo-23-3727-2005
Cornilleau-Wehrlin N, Solomon J, Korth A, Kremser G (1985) Experimental study of the relationship between energetic electrons and ELF waves observed on GEOS: a support to quasi-linear theory. J Geophys Res 90(A5):4141–4154. https://doi.org/10.1029/JA090iA05p04141
Dimmock AP, Russell CT, Sagdeev RZ et al (2019) Direct evidence of nonstationary collisionless shocks in space plasmas. Science Adv 5(2):eaau9926. https://doi.org/10.1126/sciadv.aau9926
ESA press release (2011) 'Dirty hack' restores Cluster mission from near loss. https://www.esa.int/Enabling_Support/Operations/Dirty_hack_restores_Cluster_mission_from_near_loss. Accessed 19 April 2024
ESA Re-entry Safety Requirements, ESSB-ST-U-004, 2017; https://sdup.esoc.esa.int/documents/download/ESSB-ST-U-004-Issue14December2017.pdf. Accessed 26 April 2024
ESA Policy on Space Debris Mitigation for Agency Projects, ESA-ADMIN-IPOL-2023-1. https://technology.esa.int/upload/media/ESA-ADMIN-IPOL-2023-1-Space-Debris-Mitigation-Policy-Final.pdf. Accessed 26 April 2024
Escoubet CP, Fehringer M, Goldstein M (2001) The Cluster mission. Ann Geophys 19:1197–1200. https://doi.org/10.5194/angeo-19-1197-2001
Escoubet CP, Hwang K-J, Toledo-Redondo S et al (2020) Cluster and MMS simultaneous observations of magnetosheath high speed jets and their impact on the magnetopause. Front Astron Space Sci 6:78. https://doi.org/10.3389/fspas.2019.00078
Escoubet CP, Masson A, Laakso H et al (2021) Cluster after 20 years of operations: science highlights and technical challenges. J Geophys Res Space Phys 126:e2021JA029474. https://doi.org/10.1029/2021JA029474
Faden JB, Weigel RS, Merka J et al (2010) Autoplot: a browser for scientific data on the web. Earth Sci Inform 3:41–49. https://doi.org/10.1007/s12145-010-0049-0
Fairfield DH (1971) Average and unusual locations of the Earth's magnetopause and bow shock. J Geophys Res 76(28):6700–6716. https://doi.org/10.1029/JA076i028p06700
Farris MH, Petrinec SM, Russell CT (1991) The thickness of the magnetosheath—constraints on the polytropic index. Geophys Res Lett 18:1821–1824. https://doi.org/10.1029/91GL02090
Fazakerley AN et al (2005) The double star plasma electron and current experiment. Ann Geophys 23:2733–2756. https://doi.org/10.5194/angeo-23-2733-2005
Figueiredo S, Marklund GT, Karlsson T, Johansson T, Ebihara Y, Ejiri M, Ivchenko N, Lindqvist P-A, Nilsson H, Fazakerley A (2005) Temporal and spatial evolution of discrete auroral arcs as seen by Cluster. Ann Geophys 23:2531–2557. https://doi.org/10.5194/angeo-23-2531-2005
Friis-Christensen E, Lühr H, Knudsen D, Haagmans R (2008) Swarm—an Earth observation mission investigating Geospace. Adv Space Res 41:210–216. https://doi.org/10.1016/j.asr.2006.10.008
Gabrielse C, Angelopoulos V, Runov A, Kepko L, Glassmeier KH, Auster HU et al (2008) Propagation characteristics of plasma sheet oscillations during a small storm. Geophys Res Lett 35(17):L17S13. https://doi.org/10.1029/2008GL033664
Gjerloev JW (2009) A global ground-based magnetometer initiative. Eos Trans AGU 90(27):230–231. https://doi.org/10.1029/2009EO270002
Gjerloev JW (2012) The SuperMAG data processing technique. J Geophys Res 117:A09213. https://doi.org/10.1029/2012JA017683
Green JL, Boardsen S, Garcia L, Taylor WWL, Fung SF, Reinisch BW (2005) On the origin of whistler mode radiation in the plasmasphere. J Geophys Res 110:A03201. https://doi.org/10.1029/2004JA010495
Gummow RA, Eng P (2002) GIC effects on pipeline corrosion and corrosion control systems. J Atmos Solar Terr Phys 64(16):1755–1764. https://doi.org/10.1016/S1364-6826(02)00125-6
Hietala H, Laitinen TV, Andréeová K et al (2009) Supermagnetosonic jets behind a collisionless quasi-parallel shock. Phys Rev Lett 103(24):245001. https://doi.org/10.1103/PhysRevLett.103.245001
Kepko LR, Nakamura YS et al (2024) Heliophysics Great Observatories and international cooperation in Heliophysics: an orchestrated framework for scientific advancement and discovery. Adv Space Res 73(10):5383–5405
Klein KG, Spence H, Alexandrova O et al (2023) HelioSwarm: a multipoint, multiscale mission to characterize turbulence. Space Sci Rev 219:74. https://doi.org/10.1007/s11214-023-01019-0
Kronberg EA, Hannan T, Huthmacher J et al (2021) Prediction of soft proton intensities in the near-earth space using machine learning. ApJ 921(1):76. https://doi.org/10.3847/1538-4357/ac1b30
Laakso H, Santolík O, Horne R, Kolmasova I, Escoubet P, Masson A, Taylor M (2015) Identifying the source region of plasmaspheric hiss. Geophys Res Lett 42:3141–3149. https://doi.org/10.1002/2015GL063755
Lemmens S, Merz K, Funke Q et al (2016) Planned yet uncontrolled re-entries of the Cluster-II spacecraft. Proceedings of the 7th European Conference on Space Debris, Darmstadt, Germany, 18–21 April 2017, published by the ESA Space Debris Office Ed. T. Flohrer & F. Schmitz; https://conference.sdo.esoc.esa.int/proceedings/sdc7/paper/647/SDC7-paper647.pdf

MacDonald EA, Donovan E, Nishimura Y et al (2018) New science in plain sight: citizen scientists lead to the discovery of optical structure in the upper atmosphere. Sci Adv 4(3):eaaq0030. https://doi.org/10.1126/sciadv.aaq0030
Maetschke KN, Kronberg EA, Partamies N, Grigorenko EE (2023) A possible mechanism for the formation of an eastward moving auroral spiral. Front Astron Space Sci. https://doi.org/10.3389/fspas.2023.1240081
Marklund GT, Ivchenko N, Karlsson T et al (2001) Temporal evolution of the electric field accelerating electrons away from the auroral ionosphere. Nature 414(6865):724–727. https://doi.org/10.1038/414724a
Marklund GT, Karlsson T, Figueiredo S et al (2004) Characteristics of quasi-static potential structures observed in the auroral return current region by Cluster. Nonlinear Process Geophys 11(1–12):1607–7946. https://doi.org/10.5194/npg-11-709-2004
Mauk BH, Fox NJ, Kanekal SG et al (2013) Science objectives and rationale for the radiation belt storm probes mission. Space Sci Rev 179:3–27. https://doi.org/10.1007/s11214-012-9908-y
Milan SE, Lester M (2001) Interhemispheric differences in the HF radar signature of the cusp region: a review through the study of a case example. Adv Polar Upper Atmos Res 15:159–177. https://doi.org/10.15094/00006338
Miyoshi Y, Kasaba Y, Shinohara I et al (2017) Geospace exploration project: Arase (ERG). J Phys Conf Ser 869:012095. https://doi.org/10.1088/1742-6596/869/1/012095
Nakamura R, Baumjohann W, Nakamura TKM, Panov EV, Schmid D, Varsani A et al (2021) Thin current sheet behind the dipolarization front. J Geophys Res Space Phys 126:e2021JA029518. https://doi.org/10.1029/2021JA029518
Nemecek Z, Safránková J, Prech L, Sibeck DG, Kokubun S, Mukai T (1998) Transient flux enhancements in the magnetosheath. Geophys Res Lett 25:1273–1276. https://doi.org/10.1029/98GL50873
Newell PT, Meng C-I (1988) Hemispherical asymmetry in cusp precipitation near Solstices. J Geophys Res 93:2643. https://doi.org/10.1029/JA093iA04p02643
Nishida A (1994) The Geotail mission. Geophys Res Lett 21(25):2871–2873. https://doi.org/10.1029/94GL01223
Paschmann G, Schwartz SJ, Escoubet CP, Haaland S (2005) Outer magnetospheric boundaries: cluster results, editors, ISSI Space Science Series, Springer, Reprinted from Space Science Reviews, 118: 1–4. https://doi.org/10.1007/1-4020-4582-4
Plaschke F, Hietala H, Angelopoulos V (2013) Anti-sunward high-speed jets in the subsolar magnetosheath. Ann Geophys 31:1877–1889. https://doi.org/10.5194/angeo-31-1877-2013
Rae J, Forsyth C, Dunlop M et al (2022) (2022) What are the fundamental modes of energy transfer and partitioning in the coupled Magnetosphere-Ionosphere system? Exp Astron 54:391–426. https://doi.org/10.1007/s10686-022-09861-w
Renaud F, Boily CM, Naab T, Theis C (2009) Fully compressive tides in galaxy mergers. Astrophys J 706:67–82. https://doi.org/10.1088/0004-637X/706/1/67
Retinò A, Khotyaintsev Y, Le Contel O et al (2022) Particle energization in space plasmas: towards a multi-point, multi-scale plasma observatory. Exp Astron 54:427–471. https://doi.org/10.1007/s10686-021-09797-7
Roelof EC, Sibeck DG (1993) Magnetopause shape as a bivariate function of interplanetary magnetic field Bz and solar wind dynamic pressure. J Geophys Res 98(A12):21421–21450. https://doi.org/10.1029/93JA02362
Russell CT, Elphic RC (1978) Initial ISEE magnetometer results: magnetopause observations. Space Sci Rev 22(681–715):1978. https://doi.org/10.1007/BF00212619
Sanvido S. Cluster-II end of life and re-entry assessment: Cluster-II-2 optimal maneuver re-entry analysis, ESA internal technical note, CLU-REN-TN-0377-OPS-SD, 2023.
Savin S, Amata E, Zelenyi L et al (2008) (2008) High energy jets in the Earth's magnetosheath: implications for plasma dynamics and anomalous transport. Jetp Lett 87:593–599. https://doi.org/10.1134/S0021364008110015
Sergeev V, Runov A, Baumjohann W, Nakamura R, Zhang TL, Volwerk M et al (2003) Current sheet flapping motion and structure observed by Cluster. Geophys Res Lett 30(6):1327. https://doi.org/10.1029/2002GL016500
Sergeev V, Runov A, Baumjohann W, Nakamura R, Zhang TL, Balogh A et al (2004) Orientation and propagation of current sheet oscillations. Geophys Res Lett 31:L05807. https://doi.org/10.1029/2003GL019346
Shue J-H, Chao J-K, Song P, McFadden JP (2009) Anomalous magnetosheath flows and distorted subsolar magnetopause for radial interplanetary magnetic fields. Geophys Res Lett 36:L18112. https://doi.org/10.1029/2009GL039842
Sonwalkar VS, Iman US (1989) Lightning as an embryonic source of VLF hiss. J Geophys Res 94:6986–6994. https://doi.org/10.1029/JA094iA06p06986
Southwood DJ, Farrugia CJ, Saunders MA (1988) What are flux transfer events? Planet Space Sci 36:503–508. https://doi.org/10.1016/0032-0633(88)90109-2
Thorne RM, Smith EJ, Burton RK, Holzer RE (1973) Plasmaspheric hiss. J Geophys Res 78:1581–1595. https://doi.org/10.1029/JA078i010p01581
Wei D, Dunlop MW, Yang J, Dong X, Yu Y, Wang T (2021) Intense dB/dt variations driven by near-Earth bursty bulk flows (BBFs): a case study. Geophys Res Lett 48:e2020GL091781. https://doi.org/10.1029/2020GL091781
Weigel RS, Vandegriff J, Faden J et al (2021) HAPI: an API standard for accessing Heliophysics time series data. J Geophys Res Space Phys 126:e2021029534. https://doi.org/10.1029/2021JA029534
Xiao C, He F, Shi Q et al (2023) Evidence for lunar tide effects in Earth's plasmasphere. Nat Phys 19:486–549. https://doi.org/10.1038/s41567-022-01882-8
Zhang TL, Baumjohann W, Nakamura R, Balogh A, Glassmeier K-H (2002) A wavy twisted neutral sheet observed by Cluster. Geophys Res Lett 29(19):1899. https://doi.org/10.1029/2002GL015544
Zhang X et al (2017) A new solar wind-driven global dynamic plasmapause model: 1. Database and statistics. J Geophys Res Space Phys 122:7153–7171. https://doi.org/10.1029/2022JA031232
Zhang C, Rong Z, Zhang L, Gao J, Shi Z, Klinger L et al (2023) Properties of flapping current sheet of the Martian magnetotail. J Geophys Res Space Phys 128:e2022JA031232. https://doi.org/10.1029/2022JA031232

Publisher's Note